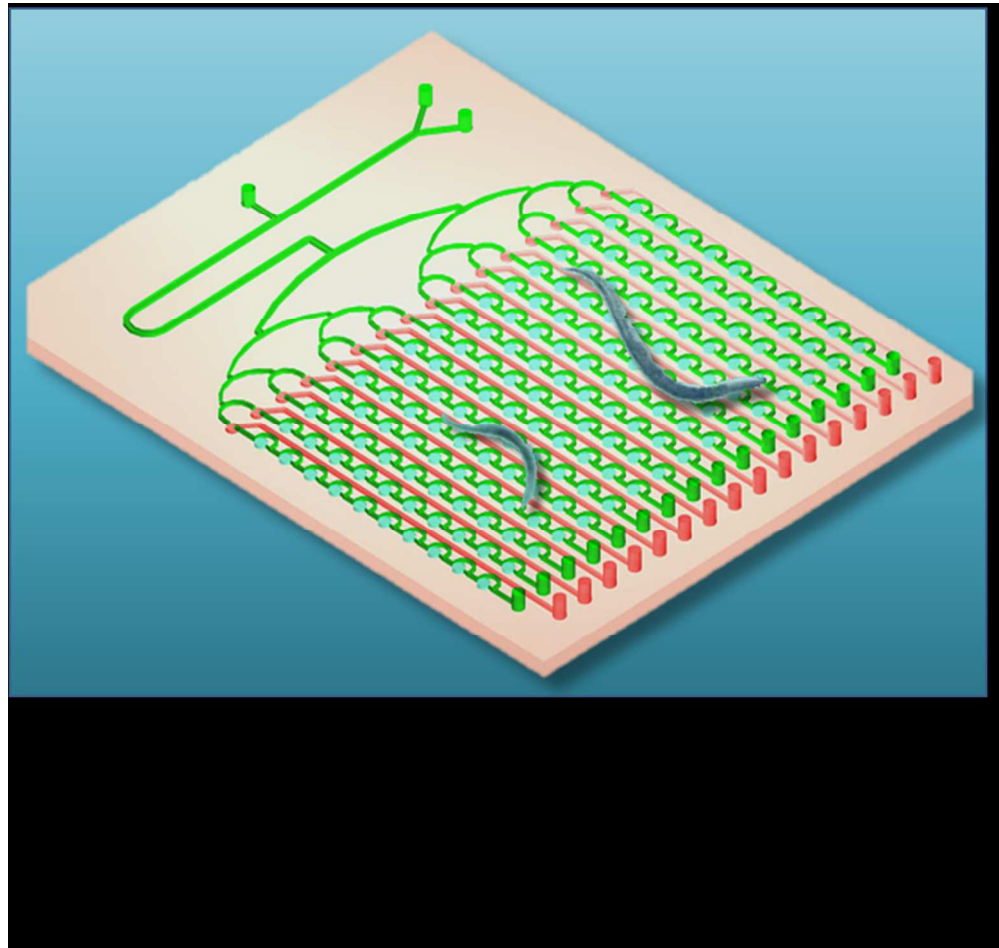




**A Droplet Microchip with Substance Exchange Capability for  
the Developmental Study of *C. elegans***

Journal:	<i>Lab on a Chip</i>
Manuscript ID:	LC-ART-11-2014-001377.R2
Article Type:	Paper
Date Submitted by the Author:	12-Feb-2015
Complete List of Authors:	Wen, Hui; Dalian Institute of Chemical Physics, Chinese Academy of Sciences, Department of Biotechnology Yu, Yue; Dalian Institute of Chemical Physics, Chinese Academy of Sciences, Department of Biotechnology Zhu, Guoli; Dalian Institute of Chemical Physics, Chinese Academy of Sciences, Department of Biotechnology Jiang, Lei; Dalian Institute of Chemical Physics, Chinese Academy of Sciences, Department of Biotechnology Qin, Jianhua; Dalian Institute of Chemical Physics, Chinese Academy of Sciences, Department of Biotechnology



a droplet microdevice was presented for post-embryonic development study of *C. elegans* initiating at L1 stage, and the effect of HIF-1 on worms development was investigated

## PAPER

# A Droplet Microchip with Substance Exchange Capability for the Developmental Study of *C. elegans*

Cite this: DOI: 10.1039/x0xx00000x

Hui Wen<sup>a#</sup>, Yue Yu<sup>a#</sup>, Guoli Zhu<sup>a</sup>, Lei Jiang<sup>a</sup>, Jianhua Qin<sup>a\*</sup>

Received 00th January 2012,

Accepted 00th January 2012

DOI: 10.1039/x0xx00000x

[www.rsc.org/](http://www.rsc.org/)

The nematode *Caenorhabditis elegans* (*C. elegans*) has been widely used as a multicellular organism in developmental research due to its simplicity, short lifecycle, and its relevance to human genetics and biology. Droplet microfluidics is an attractive platform for the study of *C. elegans* in an integrated mode with flexibility at the single animal resolution. However, it is still challenging to conduct the developmental study of worms within droplets initiating at the L1 larval stage, due to the small size, active movement, and the difficulty in achieving effective substance exchange within the droplets. Here, we present a multifunctional droplet microchip to address these issues and demonstrate the usefulness of this device for investigating post-embryonic development in individual *C. elegans* initiating at the larval L1 stage. The key components of this device consist of multiple functional units that enable parallel worm loading, droplet formation/trapping, and worm encapsulation in parallel. In particular, it exhibits superior functions in encapsulating and trapping individual larval L1 worms into droplets in a controlled way. Continuous food addition and expulsion of waste by mixing the static worm-in-droplet with moving medium plugs allows for the long-term culture of worm under a variety of conditions. We used this device to investigate the development processes of *C. elegans* in transgenic strains with deletion and overexpression of the hypoxia-inducible factor (HIF-1), a highly conserved transcript factor in regulating an organism's response to hypoxia. This microdevice may be a useful tool for the high throughput analysis of individual worms starting at the larval stage, and facilitate the study of developmental worm in response to multiple drugs or environmental toxins.

## Introduction

*Caenorhabditis elegans* (*C. elegans*) is a classical multicellular model organism used in genetics, aging, and neurobiology research.<sup>1, 2</sup> It is also a preferred model in developmental studies due to its short lifecycle, transparent body, constant cell number, and the ease with which organogenesis can be observed during the growth process.<sup>3, 4</sup> Under favorable environmental conditions, the hatched larvae are able to develop through four stages, designated stages L1 to L4 or post-embryonic developmental stages. After hatching, the germline specification in the L1 stage determines the specific behavior of cell proliferation and organogenesis during stages

L1 to L4 and in adulthood, which is of great interest in the developmental study of *C. elegans*.

It is well known that adapting to stressful environments is important for the survival of many cells and organisms, including *C. elegans*. Several stress response pathways present in *C. elegans* also exist in humans. It is recognized that the response to hypoxia plays a major role in acute injury, growth, and aging in *C. elegans*, and that a low oxygen environment activates the hypoxic response mediated by hypoxia-inducible factor (HIF-1). Previous work indicates that subjecting *C. elegans* to low oxygen conditions significantly increases the worm's lifespan. This life span extension is observed when worms are exposed to hypoxia beginning in the late larval stage and on the first day of adulthood.<sup>5</sup> Some work also shows that

genetic stabilization of the *C. elegans* HIF-1 protein (HIF-1a) under normoxic conditions is sufficient to extend the lifespan.<sup>5-7</sup> The life cycle of *C. elegans* is mainly composed of pre-adult development and adult maturation stages. However, whether or not HIF-1 has an effect on the post-embryonic development process of the worm is uncertain.

In the past decade, microfluidics technology has emerged as a promising platform for the study of *C. elegans*, both in channel-based or droplet-based formats. By providing the unique capabilities of precise manipulation and a controlled microenvironment, this platform has been used for the study of learning behavior, neurobiology, genetics, and aging processes in *C. elegans*.<sup>8-15</sup> Among these approaches, droplet microfluidics has proven to be an attractive platform for applications in worm research. This method not only provides flexible handling of individual worms in a controllable microenvironment, but also facilitates a high throughput analysis under multiple conditions. Coupled with the precise generation and manipulation of droplets of adjustable size, individual worms can be encapsulated into droplets and used in the study of worm behavior in response to various external cues. We previously proposed a droplet-microfluidics platform for worm analysis and investigated the worm's mobility behavior and neuron degeneration in response to neurotoxins in a Parkinson's disease model.<sup>16, 17</sup> Although there are prominent advantages to use the droplet-based method, it is still challenging to conduct the developmental study of larval worms within droplets, due to technical limitations. The major bottleneck lies in the difficulties in manipulating the individual worms within the droplets, initiating at the L1 stage, due to their active movement, small size, and the problems with achieving reliable substance exchanges and waste expulsion. To address these issues, we present a multifunctional droplet microdevice that is able to culture and study the post-embryonic development process in *C. elegans*, initiating at the L1 larval stage. This droplet chip allows the analysis of individual worms in a high throughput format, by integrating multiple functional components in a single device. Moreover, this integrated droplet device serves as a processor that enables continuous composite exchange by mixing the static worm-in-droplet with moving medium plugs, facilitating the study of developmental processes from L1 to the adult stage in *C. elegans* in *hif-1* and *vhl-1* mutant strains.

## Results and discussion

### Chip design

To study the developmental processes of *C. elegans* using the microdevice, it is a prerequisite to separate single L1 worms from the population, followed by subsequent culture of larval worms until adulthood. Here, we design an integrated droplet chip that allows for multiple manipulations of worm sampling, encapsulating, trapping, and long-term culturing with efficient nutrient exchange within the droplets on a single device. As shown in Fig. 1(A), the droplet chip is composed of different

functional elements, including a sample loading unit, a microvalve control unit, a 160-droplet trapping array, and a worm collection unit. The sample loading unit contains three liquid inlets and a T-junction geometry, to introduce samples and to produce plugs of fresh culture medium. The 160-droplet trap array (16 rows with 10 traps in each row) is designed to generate worms-in-droplets in a high throughput format for long-term culture. To facilitate the simultaneous analysis of multiple strains of individual worms, 16 microvalves located on the bottom control layer are used to control fluidic flow within the microchannel network that connects each row of droplet traps (Fig. 2(A)). Collecting worms at the outlet of the channel in each row makes it convenient to conduct the subsequent biochemical analysis using RT-PCR.

### Controlled generation of worm-in-droplet trap array

Fig. 1(B) illustrates the microdevice manipulation procedures used to generate a series of worms-in-droplets, followed by substance exchange within the droplets. In this experiment, fluorocarbon oil FC-40 was selected as the continuous phase due to its extraordinary biocompatibility and good solubility for oxygen. Initially, FC-40 oil was loaded into the chip to wet the surface of the PDMS microstructures and maintain its hydrophobic property. The aqueous suspension of worms was then introduced, occupying the space of the microstructures in the top fluid layer. Due to the hydrophobic property of the polydimethylsiloxane (PDMS) surface and the low viscosity of FC-40, the FC-40 oil was easily expelled from the chip, just leaving a thin film of oil on the surface of the microstructures. Then, FC-40 oil (0.001% Krytox® Performance Lubricants 157 FSL) was introduced into the chip again. As the oil phase moved forward along the microchannel, it pushed the worm suspension in the microchannel downstream and occupied the space. According to the principle of the droplet trap design,<sup>18, 19</sup> the aqueous solution entering the traps was anchored. Accordingly, in our system, the worm suspensions in the cylindrical droplet traps were not washed away by the oil phase. Instead, they split from the aqueous worm suspension bulk, forming flattened droplets and were trapped in the droplet array. The process for the worm encapsulated into droplet was shown in Supplementary materials (MovieS1). Based on the passive capture mechanism, the encapsulation efficiency for the single worm captured in single droplet was mainly affected by the worm density and flow rate of worm suspension. We optimized the experimental parameters by adjusting the worm density at 3~4 worms/ $\mu\text{L}$ , and the flow rate of worm suspension at 2 $\mu\text{L}/\text{min}$ . Under our optimized conditions, the probability for the individual L1 worm to be encapsulated into droplet was 50~60%. The images of multiple individual worms captured within separated droplets were shown in Supplementary materials (Figure S1).

To study the developmental process in the wild type N2 strain and the *hif-1* and *vhl-1* mutant strains on the same chip, we initially distributed the different worm strains into the 16 parallel arrays of droplets, aligned separately in droplet trap

rows. To control the droplets in each row individually without interference, the normally-closed microvalves were designed to manipulate the array of droplets in each row independently without cross-interference. Fig. 2 demonstrates the stepwise loading of the different ink solutions in each row. First, the microvalve in the 1st row was opened to permit the passage of fluid and the generation of trapped blue droplets. The microvalve in the second row was then opened, followed by the closure of the microvalve in the 1st row. Similarly, the trapped red droplets were generated in the 2nd row. Fig. 2(B) shows the droplets trapped in different rows could be formed independently without causing cross-contamination. In this way, the rest of the 14-row sample loading was individually controlled simply by adjusting the open-close setting on the microvalves in each row. Successive multiple sample loading into the device proves the stability of the microvalves operation. The integrated microvalves not only allow for the analysis of a single worm strain under specific conditions in a high throughput format, but also permit the analysis of different worm strains under multiple experimental conditions simultaneously.

#### Principle and validation of substance exchanges within the droplets

It has been previously reported that microfluidic droplets may provide an excellent micro-reactor for worm analysis by offering a controlled microenvironment and stable properties without external contamination.<sup>20</sup> Unlike previous work, we specifically made use of the characteristics of the unstable droplet system to realize the step-wise substance exchanges within the droplets and maintain a long-term culture of worms. The principle of substance exchange within the trapped droplets is described in Fig. 1(B). After the droplets were generated and captured in the trap array, the aqueous plugs in continuous oil phase were produced under a lower shearing force of oil at T-junction geometry in the loading unit. As the aqueous plugs passed through the traps with the captured droplets, coalescence and split between the plugs and the static droplets occurred, due to the unstable interface properties between the aqueous phase and oil phase. This process led to component exchange within the droplets. After multiple rounds of coalescence and splitting steps, complete substance replacement within the droplet was achieved.

In this system, Krytox® Perfromance 157 FSL, as a perfluoroether with carboxylic acid functionality, was added in the FC-40 oil as a surfactant. To obtain the unstable droplet system, the surfactant concentration was adjusted to 0.001wt%. It was found that a higher concentration of surfactant (e.g., 2wt %) or the absence of surfactant resulted in fusion failure or split difficulty. Under the optimized conditions of 0.001wt% surfactant, the coalescence and splitting of the trapped droplets and moving aqueous plugs occurred easily.

Fig. 3 shows the characterization of the substance exchange process within a single droplet using the fluorescent dye Rhodamine B as an indicator in aqueous plugs. During this

process, the deionized (DI) water droplet was first generated, followed by the introduction of aqueous plugs of Rhodamine B to displace the component within the droplet. The fluorescence intensity within droplets relative to the fluorescence intensity in the plugs reflected the degree of component replacement within the droplets. The time-course images of substance exchange between a moving plug of dye solution (Rhodamine B) and a single droplet of DI water are shown in Fig. 3(A). The moving aqueous plug of dye solution replaced a certain amount of liquid within the static droplet. Fig. 3(B) illustrates the distribution change of Rhodamine B in a single droplet during the substance exchange between a single droplet and 12 plugs of dye solution, until complete replacement was achieved. The substance exchange within a single droplet was accomplished within 1 min. Fig 3(C) represents the relative fluorescence intensity in a row of 10 droplets as a function of time. Sufficient substance exchanges within the droplets arranged in one row was achieved in less than 6min. The substance exchange procedure between the single droplet and multiple plugs of Rhodamine B was shown in Supplementary Materials (Movie S2).

#### Evaluation of worm growth within the individual droplets

The droplet device enables the long-term maintenance of *C. elegans* within array droplets, accompanied by sufficient component exchange and growth development from the L1 stage to adulthood. During the medium exchange within droplet, we adopted a relatively low flow velocity with the continuous phase (FC-40) at 0.75 $\mu$ L/min and the dispersed phase (medium) at 1 $\mu$ L/min, respectively. Under the optimized conditions, the appropriate length of medium plugs could be formed to facilitate the sufficient substance exchange within droplet and reduce the probability for the worms to be washed away from the anchored droplets. An approximate 90% of the individual encapsulated worms would stay in anchored droplets after the entire experimental process (from L1 to adult stage). We further reevaluated the growth status of worms cultured both in droplets and traditional well plate as well. No significant differences were observed between the two types of culture format in terms of the body length, growth rate and the stroke frequency of the worms (Supplementary materials Figure S2-4), indicating the feasibility of droplet microenvironment for normal worm culture and growth. The representative movie for cultured adult worm within droplet starting at the L1 stage was shown in Supplementary materials (Movie S3).

We further used this device to monitor worm growth during the post-embryonic development of different strains, including the wild type N2 and the transgenic strains ZG596 (*hif-1*(ia7) V) and CB5602 (*vhl-1*(ok161) X). The *hif-1* and *vhl-1* mutant strains represent worms with transgenic deletion and overexpression of *hif-1*, respectively. The expression of *hif-1* is mainly mediated by the *vhl-1/egl-9* pathway. The *vhl-1* mutation can lead to the stabilization and overexpression of *hif-1*.<sup>6</sup> The individual L1 worms of each strain were separately encapsulated into droplets on the same chip. The culture medium with food addition in

droplets was then exchanged three times every day to maintain the normal growth of the worms until they grew to adulthood (Fig.4).

During the process of worm development, body length is an important factor in evaluating growth. It has been reported that body length is associated with the regulation of several genetic pathways, such as insulin/IGF-1 (insulin-like growth factor-1) and TGF- $\beta$  (transforming growth factor- $\beta$ ) signalling.<sup>21, 22</sup> We compared the body length of worms of the different transgenic strains with or without HIF-1 expression. The body length was measured according to the curve method described previously.<sup>23</sup> As shown in Fig. 5, the *vhl-1* mutant worms (HIF-1 overexpression) exhibited short body length during the entire post-embryonic developmental process, compared with that of the wild type N2 and *hif-1* mutant worms. The percentage of worms developing into different stages initiating from the L1 stage was also evaluated. As shown in Fig. 6, the worms with the *vhl-1* mutation (HIF-1 overexpression) showed a slower growth rate than the *hif-1* mutants or the wild type N2 strain. However, there was no significant difference in growth rate between the *hif-1* mutant (HIF-1 deletion) and the wild type N2 strain. Previous work has shown that both HIF-1 deletion and overexpression extend worm lifespan under normal lab culture conditions, but through different pathways.<sup>6</sup> Coupled with previous findings, our results indicate the potential role of HIF-1 overexpression in the regulation of short body length and in the slow growth rate that occurs during post-embryonic development. This effect may also be associated with the regulating role of HIF-1 in the extension of worm lifespan. However, more work is still required to elucidate the detailed mechanism of HIF-1 involved in regulating the worm development.

## Conclusions

We describe a multifunctional droplet device that allows the investigation of developmental processes in *C. elegans*, initiating at the L1 stage. This approach enables multiple manipulations of large numbers of individual worms within droplets in a controllable way and a high throughput fashion. In particular, it permits sufficient substance exchange within the droplet by simply using continuous coalescence and splitting steps between worm-in-droplet and multiple medium plugs, facilitating the long-term culture of worm. Using this device, the worms overexpressing HIF-1 exhibited short body length with slow growth rate, indicating the potential role of HIF-1 in regulating worm development. This droplet system provides a useful platform for the long-term study of developmental worm, which can be further extended to study the worm developmental behaviors in response to multiple drugs or environmental toxins.

## Experimental

### Device fabrication

The microchip is composed of three PDMS layers, the top fluid layer, the middle PDMS membrane layer, and the bottom control layer. The microdevice was fabricated from PDMS (Sylgard 184, Dow Corning, Midland, MI) using the rapid prototyping technique.<sup>24</sup> Briefly, SU-8 3035 photoresist (Microchem, Newton, CA) was spin-coated onto glass wafers and patterned by photolithography. The structure of the fluid and the control layers were at a thickness of 200 $\mu$ m and 100 $\mu$ m, respectively. The PDMS base and the curing agents, with a mixing ratio of 10:1 by mass, were mixed, degassed under a vacuum, and poured onto the two SU-8 masters. PDMS on the SU-8 master of the control layer was spun at 600rpm for 30s. The PDMS was cured at 80°C for 45min. The flow layer was then peeled off from the SU-8 master and subsequently bonded to the PDMS cover on the control layer SU-8 master after plasma treatment. The two-layer PDMS replica was peeled off from the control layer SU-8 master immediately. Finally, the replica was bonded to a glass wafer with plasma treatment.

### Worm strains and maintenance

The wild type N2 strain and transgenic worm strains ZG596 (*hif-1(ia7)V*) and CB5602 (*vhl-1(ok161)X*) were obtained from the *Caenorhabditis* Genetics Centre at the University of Minnesota (St. Paul) and cultivated as described by Brenner.<sup>25</sup> Briefly, the worms were cultivated at 20°C on a nematode growth medium (NGM) agar seeded with *Escherichia coli* OP50 (food). Prior to seeding, bacteria were incubated overnight at 37°C and stored at 4°C.

### Operation of the integrated droplet device

Synchronized L1 worms of the three strains were washed into K medium (50mM NaCl, 30mM KCl, 10mM NaOAc, pH 5.5) with *E. coli* from agar plates at 20°C. The density of the worm suspension was adjusted to 3~4 worms/ $\mu$ L. The worm suspension was then introduced onto the chip (the chip had been filled with FC-40 oil prior to this) through the worm inlet, with a flow velocity of 2 $\mu$ L/min using a syringe pump. During the injection, the other two inlets were blocked. After the worm suspension filled up all of the space of the microstructures in the top fluid layer, the syringe pump was stopped. Immediately afterwards, FC-40 oil (0.001% Krytox<sup>®</sup> Performance Lubricants 157 FSL) was introduced into the chip through the oil inlet (2 $\mu$ L/min) to expel the worm suspension that resided in the microchannel, leaving the worm suspension in the traps behind to form droplet arrays.

To achieve food addition in the droplets, K medium solution with food was introduced through the medium inlet, in which the OD value of the medium containing *E. coli* OP50 equaled 0.6. At the same time, the FC-40 oil was continuously introduced. In such a case, the aqueous plugs of K medium in continuous oil phase were generated under the shearing force of the oil at the T-junction geometry in the loading unit (The flow velocity of K medium and oil were 0.75  $\mu$ L/min and 1 $\mu$ L/min, respectively). When the aqueous plugs passed by the droplets that were detained in the traps, coalescence and split between

the plug and droplet would occur, causing the exchange of substances within droplet after the repeated procedures followed by food addition and waste expulsion. Normally, the normally-closed microvalves are open during each of these procedures, and the valves are closed after the operations are finished. To collect the worms for subsequent assay, the microfluidic channel was washed with medium using syringe pumps to make the worm flushed from the outlet of the chip into the centrifuge tube separately.

## Acknowledgements

This research was supported by the Key Laboratory of Separation Sciences for Analytical Chemistry, Dalian Institute of Chemical Physics, CAS, the National Nature Science Foundation of China (No.81273483, No.31171149), and the International Science & Technology Cooperation Program of China (ISTCP) (S2015ZR1058).

## Notes and references

<sup>a</sup> Division of Biotechnology, Dalian Institute of Chemical Physics, Chinese Academy of Sciences

<sup>#</sup> These authors contributed equally to this work and should be considered co-first authors.

<sup>†</sup> Footnotes should appear here. These might include comments relevant to but not central to the matter under discussion, limited experimental and spectral data, and crystallographic data.

Electronic Supplementary Information (ESI) available: [details of any supplementary information available should be included here]. See DOI: 10.1039/b000000x/

1. P. Sengupta and A. D. Samuel, *Current Opinion in Neurobiology*, 2009, **19**, 637.
2. P. Reis-Rodrigues, G. Czerwieniec, T. W. Peters, U. S. Evani, S. Alavez, E. A. Gaman, M. Vantipalli, S. D. Mooney, B. W. Gibson, G. J. Lithgow, and R. E. Hughes, *Aging Cell*, 2012, **11**, 120.
3. Y. Fuchs and H. Steller, *Cell*, 2011, **147**, 742-758.
4. D. V. Tobin and R. M. Saito, *Cell Cycle*, 2012, **11**, 1666.
5. R. Mehta, K. A. Steinkraus, G. L. Sutphin, F. J. Ramos, L. S. Shamieh, A. Huh, C. Davis, D. Chandler-Brown, and M. Kaeberlein, *Science*, 2009, **324**, 1196.
6. Y. Zhang, Z. Shao, Z. Zhai, C. Shen, and J. A. Powell-Coffman, *PLoS One*, 2009, **4**, e6348.
7. R. U. Muller, F. Fabretti, S. Zank, V. Burst, T. Benzing, and B. Schermer, *Journal of the American Society of Nephrology: JASN*, 2009, **20**, 2513.
8. A. San-Miguel and H. Lu, *Worm Book: the Online Review of C. elegans Biology*, 2013, DOI: 10.1895/wormbook.1.162.1, 1.
9. S. X. Guo, F. Bourgeois, T. Chokshi, N. J. Durr, M. A. Hilliard, N. Chronis, and A. Ben-Yakar, *Nature Methods*, 2008, **5**, 531.
10. H. Ma, L. Jiang, W. Shi, J. Qin, and B. Lin, *Biomicrofluidics*, 2009, **3**, 44114.
11. S. E. Hulme, S. S. Shevkoplyas, A. P. McGuigan, J. Apfeld, W. Fontana, and G. M. Whitesides, *Lab on a Chip*, 2010, **10**, 589.
12. K. Chung, M. Zhan, J. Srinivasan, P. W. Sternberg, E. Gong, F. C. Schroeder, and H. Lu, *Lab on a Chip*, 2011, **11**, 3689.
13. H. Wen, W. Shi and J. Qin, *Biomedical Microdevices*, 2012, **14**, 721.
14. J. Larsch, D. Ventimiglia, C. I. Bargmann, and D. R. Albrecht, *Proceedings of the National Academy of Sciences of the United States of America*, 2013, **110**, E4266.
15. H. Wen, X. Gao, and J. Qin, *Integrative Biology*, 2014, **6**, 35.
16. W. Shi, J. Qin, N. Ye, and B. Lin, *Lab on a Chip*, 2008, **8**, 1432.
17. W. Shi, H. Wen, Y. Lu, Y. Shi, B. Lin, and J. Qin, *Lab on a Chip*, 2010, **10**, 2855.
18. H. Boukellal, S. Selimovic, Y. Jia, G. Cristobal, and S. Fraden, *Lab on a Chip*, 2009, **9**, 331.
19. M. Sun, S. S. Bithi, and S. A. Vanapalli, *Lab on a Chip*, 2011, **11**, 3949.
20. M. Xie and R. Roy, *Cell Metabolism*, 2012, **16**, 322.
21. S. So, K. Miyahara, and Y. Ohshima, *Genes to Cells: Devoted to Molecular & Cellular Mechanisms*, 2011, **16**, 639.
22. J. Wang, R. Tokarz, and C. Savage-Dunn, *Development*, 2002, **129**, 4989.
23. C. Morck and M. Pilon, *BMC Developmental Biology*, 2006, **6**, 39.
24. J. C. McDonald, D. C. Duffy, J. R. Anderson, D. T. Chiu, H. Wu, O. J. Schueller, and G. M. Whitesides, *Electrophoresis*, 2000, **21**, 27.
25. S. Brenner, *Genetics*, 1974, **77**, 71.

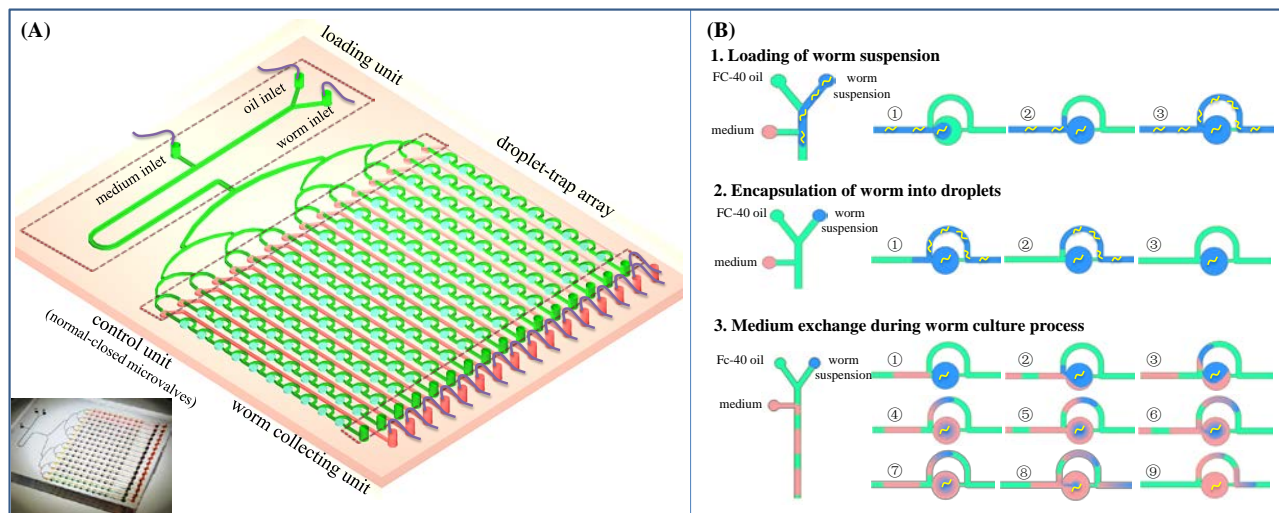


Figure 1. Schematic and operation of the droplet chip for *C. elegans* developmental study. (A) Schematic diagram and photograph of the droplet chip. (B) Flow chart illustrating individual worm encapsulation and substance exchanges within the droplets for long-term culture. Step one: loading of worm suspension and expulsion of FC-40 oil from the microchannel and droplet trap. Step two: loading of FC-40 oil, expulsion of the worm suspension out of the main channel, and maintenance of the worm suspension in the droplet trap to form worm-encapsulated droplets. Step three, complete medium exchange in droplets was achieved after several rounds of coalescence and splitting between the droplets and medium plugs.

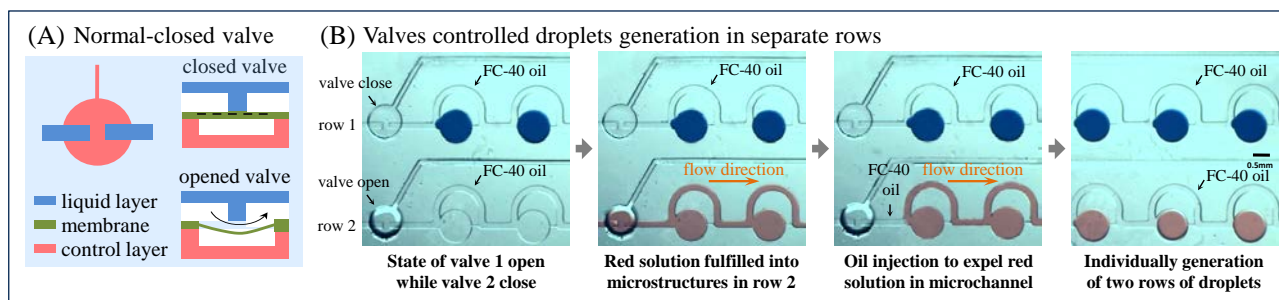


Figure 2. Illustration of microvalve controlled droplet manipulation in separated rows. (A) Schematic diagram of normal-closed valve, in which the microvalve is activated by applying a vacuum in the bottom control layer. (B) The two rows of array droplets are generated and controlled independently without interference.



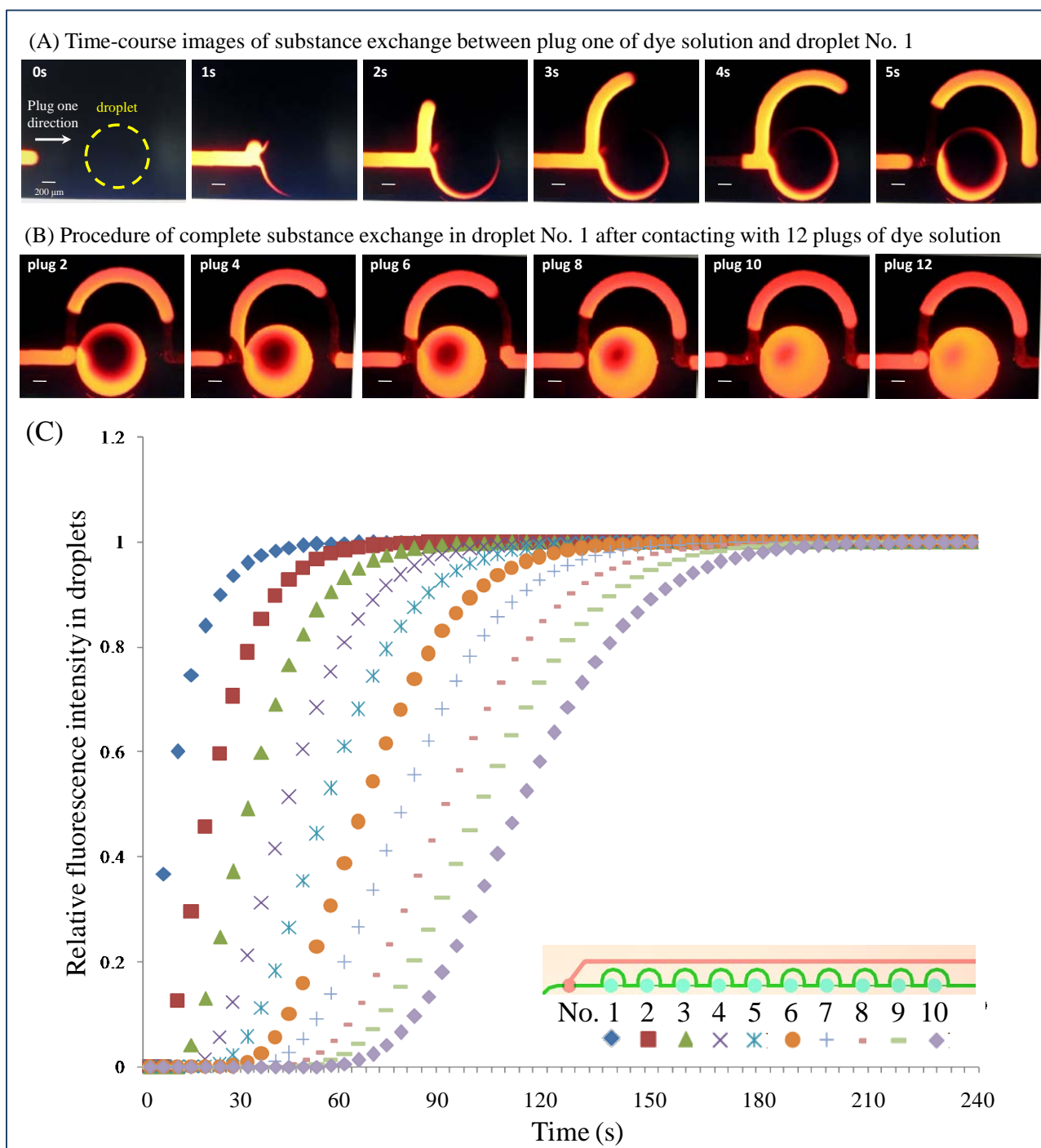


Figure 3. Characterization of the substance exchange between the single droplet and plugs of dye solution. (A) Time course images of the coalescence and splitting process between the first generated aqueous droplet (DI water) and the aqueous plug (Rhodamine B). (B) Images of substance exchange occurring in droplet No. 1 after continuous contact with 12 plugs of Rhodamine B solution. (C) Quantitative evaluation of fluorescence intensity of Rhodamine B within 10 droplets of one row on the device.

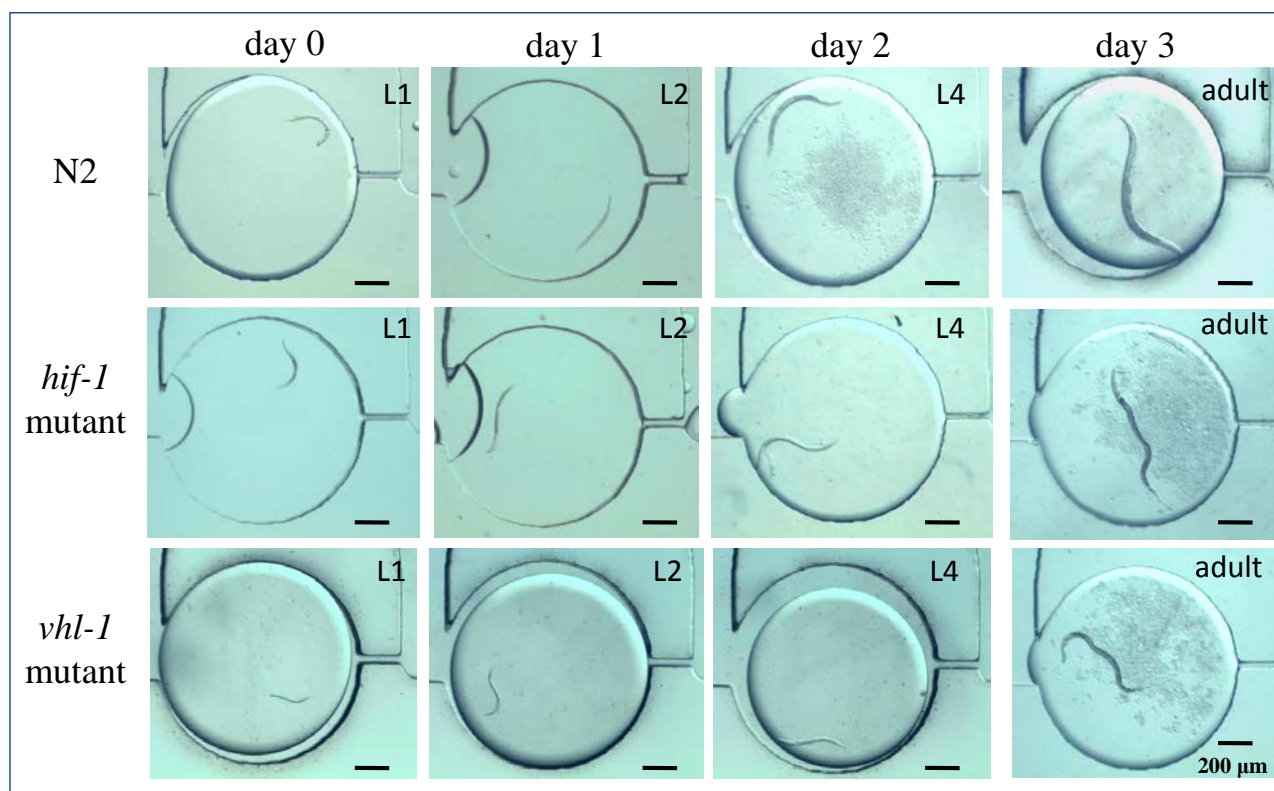


Figure 4. Time-course images of worm growth within a single droplet for the wild type N2 strain and the *hif-1* and *vhl-1* mutant worm strains. The worms were cultured at 20°C under normoxic conditions. The nutrient exchanges with food addition within the droplets were carried out three times each day.

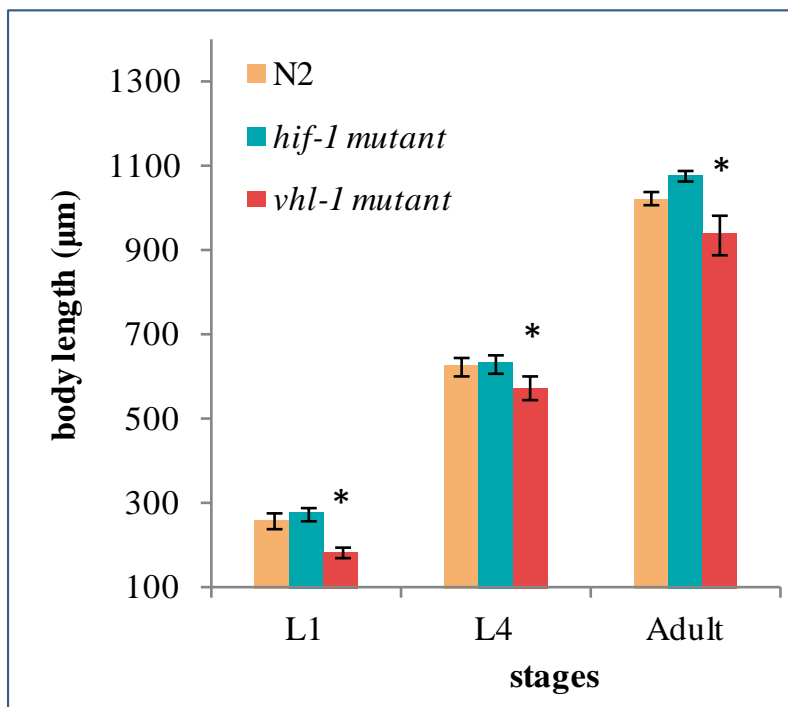


Figure 5. Comparison of worm body length across the post-embryonic developmental stages in wild type N2, *hif-1* mutant, and *vhl-1* mutant worm strains. The worms were cultured at 20°C under normoxic conditions. The error bars indicate the SEM (n=20, N=3) relative to the control: \*p<0.05.

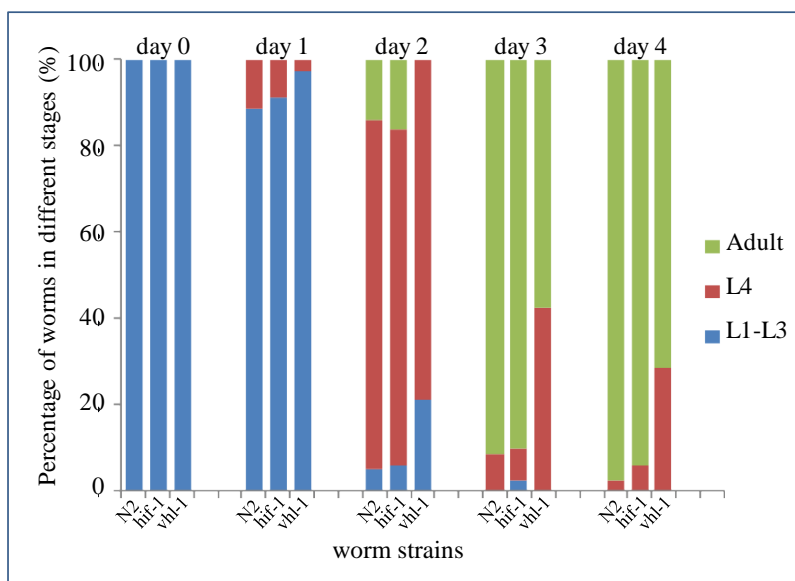


Figure 6. Percentage of different worm strains in post-embryonic stages over time. The wild type N2, *hif-1* mutant, and *vhl-1* mutant worm strains were cultured at 20°C under normoxic conditions.